Initial Surface Roughening in Ge/Si(001) Heteroepitaxy Driven by Step-Vacancy Line Interaction

P. Sutter, I. Schick, W. Ernst, and E. Sutter
Department of Physics, Colorado School of Mines, Golden, Colorado 80401, USA
(Received 28 May 2003; published 23 October 2003)

The initial surface roughening during Ge epitaxy on Si(001) is shown to arise from an effective repulsion between S_A surface steps and dimer vacancy lines (VLs). This step-VL interaction gradually inactivates a substantial fraction of adatom attachment sites at the growth front, causing a rapid increase in the rate of two-dimensional island nucleation. The mutual repulsion hinders the crossing of S_A surface steps over VLs in the second layer, thus organizing the developing surface roughness into a periodic array of anisotropic 2D terraces. Isolated (105) facets forming at specific sites on this ordered template mediate the assembly of first 3D Ge islands.

DOI: 10.1103/PhysRevLett.91.176102 PACS numbers: 68.55.Ac, 68.37.Ef, 81.15.–z, 81.16.Rf

Ge and $Si_{1-x}Ge_x$ thin films on Si(001) have long served as a model system for strained-layer heteroepitaxy, and have shown a surprisingly rich sequence of morphological transformations. They include the formation and ordering of surface defects (dimer vacancies [1]), the transition to three-dimensional (3D) growth in the form of shallow faceted, coherent islands [2], and transformations of the shape of these islands with increasing volume [3]. Potential applications of 3D Ge "quantum dots" depend critically on an understanding of the morphological evolution leading to the first faceted islands. Processes at the early growth stages may promote size uniformity or long-range ordering of the islands, both of which are important prerequisites for technological applications.

In Ge (or $Si_{1-x}Ge_x$) epitaxy on Si(001) the first faceted 3D islands do not form on a planar "wetting layer," but on a template of correlated roughness [4,5] generated at low coverage. Though observed routinely [4,6], the progressive roughening of an ultrathin Ge layer, which even at high substrate temperatures involves a rapid transition from step-flow to layer-by-layer growth, remains poorly understood. Roughening has been interpreted as a strain relaxation mechanism [7], intermediate between the generation of dimer vacancy lines (VLs) at submonolayer (ML) coverage and the formation of (105) faceted 3D islands at about 4 ML. This scenario assumes that shallow surface undulations, possibly in the form of ordered "stress domains" [8], are energetically favorable over a planar strained surface. However, alternative explanations for the observed roughening are possible. A potential role of growth kinetics, likely involving the VLs partitioning the growth front into a well-ordered $2 \times N$ reconstruction, has long been suggested [6] but was never confirmed.

In this Letter we use the combination of epitaxial growth and scanning tunneling microscopy (STM) to study the initial roughening of thin Ge films on Si(001). We have developed the capability of obtaining atom-resolved STM images of very large sample areas, thus achieving an unprecedented combination of image statistics and detail across all length scales relevant to epitaxy. Using this novel experimental capability in conjunction with a careful statistical analysis of characteristic morphological features, we identify a pronounced short-range repulsion between advancing surface steps and VLs in the underlying terraces. This interaction poses a substantial kinetic limitation to step flow. It slows the incorporation of adatoms into existing steps, promotes a rapid increase in the rate of 2D nucleation, and thus drives the roughening of the growing Ge film in the form of highly correlated features whose dimensions are well defined on the atomic scale. The resulting surface roughness can provide sites for the generation of oblique (105) facets, thus facilitating the formation of 3D islands. Our findings provide a long-sought coherent framework for the transformation from a 2D wetting layer to 3D islands in the $Si_{1-x}Ge_x$/Si(001) system, which for the entire composition range associated with island growth ($\sim 0.1 \leq x \leq 1$) involves a gradual buildup of roughness and spontaneous (105) faceting at sites providing a critical slope relative to the (001) surface [9].

Our growth experiments were performed by magnetron sputter epitaxy [10] on vicinal Si(001) substrates with 0.14° miscut along [110]. The substrates were cleaned by thermal desorption of the native oxide at 1250 °C [11], which results in a well-ordered surface structure with very low contaminant density as shown by STM. Ge was deposited to coverages up to 5 ML at temperatures T between 450 °C and 650 °C, and at a growth rate $R = 0.1$ ML/s. As-grown samples were quenched to ambient T and transferred *in situ* to an ultrahigh-vacuum STM operating at 5×10^{-11} Torr. Large-area STM scans with fields of view of up to 1 μm^2 and atomic resolution at a typical pixel spacing of 0.05 nm were used to map the surface morphology of the epitaxial Ge layers across multiple length scales. Such large scans were obtained at room temperature in a homebuilt, isothermally shielded STM with very low tip-sample drift, using a

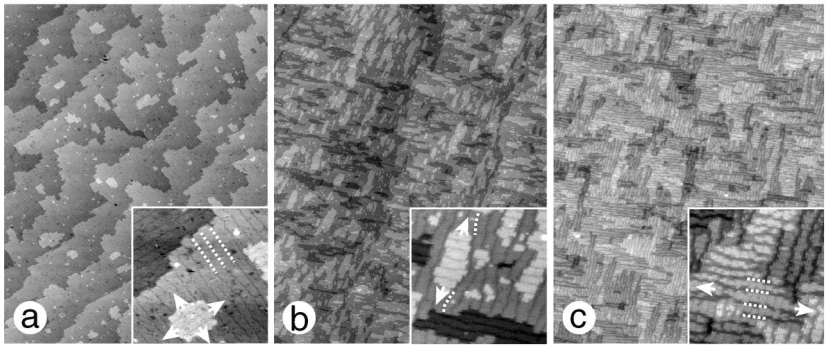

FIG. 1. Surface morphology evolution during Ge growth on Si(001) at $T = 550\,^{\circ}\mathrm{C}$. Large-area atom-resolved STM images (400 nm × 500 nm): (a) 1.5 ML, (b) 2.3 ML, and (c) 3.5 ML Ge coverage. Insets are close-up views (50 nm × 50 nm), showing the positions of representative VLs (dashed lines) and the directions of preferential 2D island expansion (arrows).

digital signal processor-based controller capable of acquiring up to 2^{15} pixels per scan line [12].

Figure 1 shows the surface morphology evolution with increasing coverage during Ge growth on Si(001) at 550 °C. Starting with a staircase of (001) terraces separated by alternating S_A and S_B steps [13], Ge growth drives the formation of lines of dimer vacancies at sub-ML coverage. Previous studies have shown that the VLs interact elastically via an effective potential that is attractive at large separation and repulsive at small spacing [14], and whose minimum gives rise to a well-defined equilibrium separation and pronounced ordering of the VLs [15]. We find that at 1.5 ML Ge coverage [Fig. 1(a)] the VLs are fairly well ordered, with a distance distribution that peaks at about $9a_0$, where $a_0 = 0.381$ nm. Real-time observations of Ge/Si(001) epitaxy by low-energy electron microscopy show step-flow growth at the onset of Ge deposition at sub-ML coverage under conditions similar to those used here ($R = 0.1$ ML/s; $T = 550\,^{\circ}\mathrm{C}$). At the higher coverage shown in Fig. 1(a), Ge growth is no longer by step flow alone [16], but it involves the nucleation of 2D terraces. These 2D islands are roughly square-shaped, i.e., have aspect ratios close to 1. Their dimensions often exceed the VL spacing. During growth from an atomic-scale critical nucleus their S_A step segments must have "crossed" VLs in the underlying terrace.

With increasing Ge coverage a rapid transition in the growth mode takes place. The flow of substrate steps ceases and the nucleation rate and density of 2D islands increase. Figure 1(b) shows the surface morphology at 2.3 ML Ge coverage. Newly formed 2D islands are now narrower and longer, reaching aspect ratios between 3 and 6. A large fraction of these islands has still expanded beyond the VL spacing. At even higher Ge coverage [Fig. 1(c)], the trend to higher 2D island density continues, leading to surface roughness in the form of a periodic patchwork of strongly anisotropic terraces (aspect ratio up to 30), separated by ML deep trenches. Each of these trenches contains a single VL, and virtually *all* 2D islands observed in Fig. 1(c) are confined between two adjacent VLs in the underlying terrace. The island width thus saturates at a well-defined value of $\sim 8a_0$, given by the separation of dimer vacancy lines in the second layer.

Progressive surface roughening and an increase in 2D island density with Ge coverage may be caused by a number of factors, e.g., a reduction in surface diffusion length with increasing Ge coverage. Our observations suggest a different roughening mechanism involving VLs at the Ge growth front. The inset of Fig. 1(b), a close-up of the surface at 2.3 ML Ge coverage, shows all S_A steps bounding 2D islands in close proximity to a parallel VL on the underlying terrace. S_A steps and VLs meander laterally. Their short-range meandering is highly correlated, with a linear correlation of 92% between S_A step and VL positions. The distance distribution of S_A steps and adjacent VLs was analyzed, as shown in Fig. 2. A continuous replenishing of the adatom reservoir by condensing Ge vapor is expected to advance both types of surface steps (S_A, S_B). In the absence of an interaction between advancing S_A steps and underlying VLs, a flat

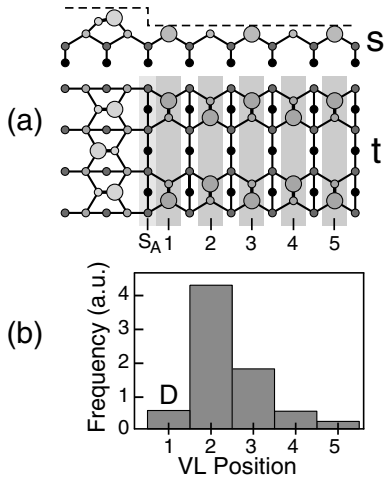

FIG. 2. (a) Ball-and-stick model (s: side view; t: top view) of the atomic structure near an S_A step. (b) Statistical analysis of the separation of VLs and adjacent S_A steps for 2.3 ML Ge/Si(001). Possible VL positions are labeled 1 through 5. A VL at position 1 creates a D_A-type double height step (D).

S_A-VL distance distribution would be expected, i.e., none of the possible S_A-VL configurations should be preferred. The measured distribution [Fig. 2(b)], however, peaks sharply for S_A steps and VLs in configuration 2, for which the VL is separated by only one dimer from the advancing S_A step. Larger separations (configuration 3 and beyond) are less likely, indicating that the growth flux rapidly drives the step out of these configurations. And configuration 1, in which step and VL merge to form a double-layer D_A step, is substantially less probable, in agreement with calculations, which—albeit for Si(001)—give a D_A step free energy that is considerably higher than for a pair of single-layer S_A and S_B steps [13].

The reluctance to form double-layer steps and to "fill in" (annihilate) VLs can give rise to a pronounced short-range repulsion between advancing S_A steps and VLs [17]. STM scans of large sample areas at full atomic resolution allowed us to statistically analyze rare "tell-tale" morphological features, and thus obtain evidence for the existence of such an interaction. For 2.3 ML Ge coverage, we have analyzed the spacing of pairs of VLs in the second layer for three distinct configurations (Fig. 3). The "free" configuration denotes pairs of VLs far from, i.e., not influenced by, any S_A steps. The "stretched" configuration involves a pair of VLs with a new 2D terrace growing between them. The "squeezed" configuration, finally, consists of a pair of VLs confined between S_A edges of two adjacent 2D terraces. The analysis of several thousand free, and several hundred stretched and squeezed vacancy line spacings, is summarized in Fig. 3.

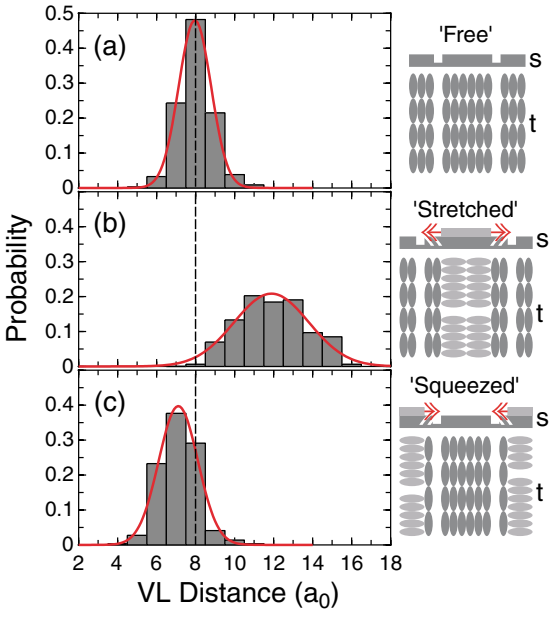

FIG. 3 (color online). Statistical analysis of the separation of VL pairs for 2.3 ML Ge/Si(001) in three configurations: (a) "free," far from S_A steps; (b) "stretched," with a pair of S_A steps moving outward between adjacent VLs; (c) "squeezed," with two S_A steps moving inward toward a pair of VLs. Lines represent Gaussian fits to the data. Sketches of the VL-step configurations are shown next to the histograms (s: side view; t: top view).

In the free configuration, the average VL spacing is $(8.0 \pm 0.9)a_0$, in good agreement with values obtained previously [1,18]. A reduced spacing compared to 1.5 ML Ge coverage [Fig. 1(a)] is consistent with the general trend to smaller VL separation with increasing coverage [18]. We find a narrower distribution than other groups [18], likely due to the superior statistics obtained from our large-area STM images. The stretched configuration shows a substantial increase in the average VL separation to $(11.9 \pm 1.7)a_0$. Conversely, the average spacing in the squeezed configuration is reduced to $(7.1 \pm 0.9)a_0$. These results confirm a short-range repulsion between advancing S_A steps and VLs in the underlying terrace, altering the equilibrium separation of adjacent VLs. In the stretched configuration, the effective force on a VL due to an advancing S_A step counteracts the weak VL-VL attraction, and can substantially increase the spacing between two VLs. In the squeezed configuration the effective S_A-VL interaction potential acts against the strong VL-VL repulsion, resulting in a smaller reduction of the spacing of the VL pair.

In Si homoepitaxy on Si(001) S_B steps are efficient sinks for adatoms, with an incorporation rate exceeding that of S_A steps roughly tenfold [19]. On vicinal Si(001) this incorporation asymmetry causes the formation of a nearly single-domain (2×1) surface in step-flow growth [19]. Real-time observations of step flow in the presence of Ge show equally sized (2×1) and (1×2) domains, i.e., symmetric S_A and S_B incorporation, suggesting that Ge alters the step attachment kinetics. Assuming that S_A and S_B are symmetric adatom sinks during Ge/Si(001) growth, the termination of S_A step flow due to an effective S_A-VL repulsion inactivates roughly half of the incorporation sites at existing step edges. The step-VL interaction thus gives rise to a substantially increased adatom concentration on the terraces, leading to a rise in 2D island nucleation rate, and causing the observed rapid transition to 2D island growth and roughening of the growth front. The effective S_A-VL repulsion appears to strongly depend on Ge coverage. At low coverage [Fig. 1(a)], 2D nuclei typically "cross" several underlying VLs. At high Ge coverage [Fig. 1(c)], such crossing is virtually inhibited and all 2D islands are rigidly confined between adjacent VLs in the second layer. This coverage dependence may result from a progressive increase in Ge concentration at the growth front as intermixing with the Si substrate diminishes gradually [16], and associated strengthening of the effective S_A-VL repulsion. In its final stage, surface roughening due to S_A-VL interaction gives rise to a pronounced self-organization of the growth front into a periodic array of anisotropic 2D islands whose width is limited by the VL-VL separation.

We now turn to a brief discussion of how this correlated wetting layer roughness influences the subsequent formation of (105) faceted "hut" islands (Fig. 4). At first

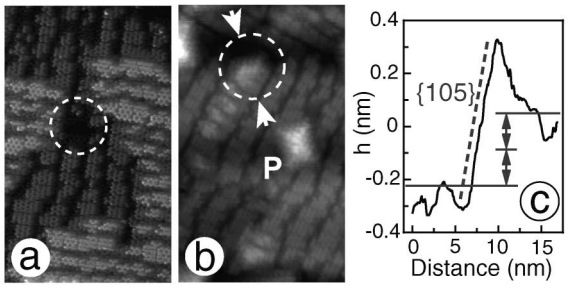

FIG. 4. STM images (50 nm × 30 nm) showing the onset of (105) faceting and 3D "hut" island formation on a template of correlated roughness near 4 ML Ge coverage (a) 3.5 ML Ge/Si(001): elongated top-layer terraces, confined between second-layer VLs. Statistically distributed deeper depressions (circle). (b) 4.0 ML Ge/Si(001): rebonding and creation of an isolated (105) facet at a substrate depression (circle). Somewhat larger 3D structures (P, 3 ML tall) are pyramid-shaped. (c) Line profile between arrows in (b), showing a local accumulation of material and formation of a microscopic (105) facet into the 2 ML deep depression.

sight, the roughness could be interpreted as the analog of a larger patchwork of stepped mounds observed in $Si_{1-x}Ge_x$ alloy epitaxy on Si(001), which serves as a template for (105) faceted 3D islands during alloy growth [5]. The periodicity of the cell structure on a Ge wetting layer, as observed here, would then imply the potential for the spontaneous generation of periodic arrays of 3D Ge islands. We find, however, that the system takes a different route to (105) faceting. The trenches separating elongated 2D islands are shallow (2 ML deep), and align with [110] zone axes. They do not trigger any (105) faceting. Instead, the first oblique facets appear to form at spontaneously generated, statistically distributed deeper surface depressions [Fig. 4(a)]. These depressions, roughly circular with a typical radius below 2 nm, provide sites with higher local vicinality and, importantly, edges with average [010] orientation. Previous real-time STM studies have shown statistical fluctuations resulting in ML-high Ge accumulations at the edges of surface depressions [20]. Our images show the formation of isolated small (105) facets at these sites [Figs. 4(b) and 4(c)], analogous to the faceting pathway in $Si_{1-x}Ge_x/Si(001)$ growth [9]. Once a microscopic (105) facet is formed, it likely serves as the nucleus for a small (105) faceted pyramid [9]. All larger 3D features observed are indeed pyramid-shaped. After the formation of a sparse array of initial pyramids, additional clusters are increasingly generated by "attachment" to existing islands [21]. Invariably, however, the smallest isolated 3D objects are microscopic (105) facets whose rebonding is initiated at edges of depressions in the rough wetting layer.

In conclusion, we have identified the mechanism underlying the atomic-scale roughening of a thin Ge layer grown on Si(001). The surface roughens due to an effective repulsion between S_A surface steps and dimer vacancy lines. This interaction gradually inactivates a substantial fraction of the adatom attachment sites at the growth front, thus increasing the 2D island nucleation rate. And it hinders the crossing of S_A steps over vacancy lines in the second layer, thus organizing the surface into a periodic array of anisotropic 2D islands whose width is well defined at the atomic scale. Individual (105) facets, generated at statistically distributed depressions in this periodic structure, mediate the initial assembly of 3D Ge islands at the surface. This observation provides a coherent framework for the initial formation of quantum dot islands in $Si_{1-x}Ge_x/Si(001)$ epitaxy, which invariably proceeds from isolated (105) facets generated at sites with critical slope and [010] edge orientation on a rough template.

This work is supported by NSF under Grants No. DMR-0208673 and No. DMR-9985178. The low-energy electron microscope facility at the University of Wisconsin is supported by NSF and ONR.

[1] U. Köhler *et al.*, Ultramicroscopy **42–44**, 832 (1992).
[2] Y.-W. Mo *et al.*, Phys. Rev. Lett. **65**, 1020 (1990).
[3] F. M. Ross, R. M. Tromp, and M. C. Reuter, Science **286**, 1931 (1999).
[4] A. Vailionis *et al.*, Phys. Rev. Lett. **85**, 3672 (2000).
[5] P. Sutter and M. G. Lagally, Phys. Rev. Lett. **84**, 4637 (2000); R. M. Tromp, F. M. Ross, and M. C. Reuter, Phys. Rev. Lett. **84**, 4641 (2000).
[6] M. G. Lagally, Jpn. J. Appl. Phys. **32**, 1493 (1993).
[7] B. Voigtländer and M. Kästner, Phys. Rev. B **60**, R5121 (1999).
[8] F. Wu and M. G. Lagally, Phys. Rev. Lett. **75**, 2534 (1995).
[9] P. Sutter, P. Zahl, and E. Sutter, Appl. Phys. Lett. **82**, 3454 (2003).
[10] P. Sutter, Ph.D. thesis, Eidgenössische Technische Hochschule (ETH) Zürich, 1996.
[11] B. S. Swartzentruber *et al.*, J. Vac. Sci. Technol. A **7**, 2901 (1989).
[12] STM design and performance, P. Sutter *et al.* (to be published). For a description of the control hardware and software, see http://gxsm.sourceforge.net/.
[13] D. J. Chadi, Phys. Rev. Lett. **59**, 1691 (1987).
[14] J. Tersoff, Phys. Rev. B **45**, 8833 (1992).
[15] F. Liu and M. G. Lagally, Phys. Rev. Lett. **76**, 3156 (1996).
[16] Mixed Si-Ge step flow due to displacive adsorption; see R. M. Tromp, Phys. Rev. B **47**, 7125 (1993).
[17] In addition to S_A steps, 2D islands are bounded by S_B step segments parallel to VLs in the upper terrace. A S_B-VL interaction constrains the meandering of S_B steps [18]. Anisotropic 2D island shapes [Fig. 1(c)] suggest that, unlike S_A step flow, S_B step advances are not limited by interaction with VLs.
[18] F. Wu, X. Chen, Z. Zhang, and M. G. Lagally, Phys. Rev. Lett. **74**, 574 (1995).
[19] Y.-W. Mo *et al.*, Phys. Rev. Lett. **63**, 2393 (1989).
[20] D. E. Jesson, M. Kästner, and B. Voigtländer, Phys. Rev. Lett. **84**, 330 (2000).
[21] D. E. Jesson *et al.*, Phys. Rev. Lett. **77**, 1330 (1996).